

ICSV14

Cairns • Australia

9-12 July, 2007



THE DESIGN OF MOTOR BRACKETS FOR THE REDUCTION OF STRUCTURE-BORNE NOISE IN PACKAGE AIR-CONDITIONERS

Sang-Gil Park¹, Hyun-Jin Sim, Hae-Jin Lee¹, You-Yub Lee² and Jae-Eung Oh³

¹ Department of Mechanical Engineering, Hanyang University
Haengdang-Dong 17, Sungdong-Gu, Seoul, KOREA

² Division of Automotive & Mechanical Eng, Howon University
727, Wolha, Impi, Gunsan, Jeonbuk, KOREA

³ School of Mechanical Engineering, Hanyang University
Haengdang-Dong 17, Sungdong-Gu, Seoul, KOREA
jeoh@hanyang.ac.kr (e-mail address of lead author)

Abstract

As economic power increases and customer demand becomes more difficult to satisfy, noise and vibration will be the most important factors in determining product quality. With a sudden increase in demand, product quality and noise are becoming decisive factors in determining whether a product is purchased. Consequently, manufactures are investing significant money and research to reduce the unpleasantness of noise and vibration. In addition, they are distinguishing their products by aggressively advertising their low-noise output. For these reasons, the demand for a silent indoor air-conditioner has made relevant research essential to product development. In this study, noise and vibration are visualized in space and frequency domains by using experimental methods such as operational deflection shape (ODS), modal testing, and sound intensity. Also, the location of the noise source and its characteristics are analyzed from an acoustical point of view to reduce the structure-borne noise that comes from the fan motor, and a pertinent control method is suggested. Furthermore, the most suitable shape of the motor bracket is suggested by applying FEM and DOE (Design of experiments) from the point of view of noise and vibration.

1. INTRODUCTION

With a greater focus on environmental problems, the government is strengthening restrictions on noise, increasing the need for research in noise reduction. Because of economic growth and lifestyle changes, home appliances are the fastest growing technology for noise reduction. Also, as market competition grows fiercer among manufacturers, companies are investing millions of dollars in R&D. Among home appliances, the demand for air conditioners is rising rapidly because of income increases and changes in housing preferences. Because the rise in demand has made operational noise a more important consideration for customers, noise reduction is now as important as high efficiency and is becoming a major criterion in purchasing air-conditioners (AC).

For instance, in Korea, research on AC focused mostly on raising the heat exchange efficiency between indoor units and outdoor units, without much consideration for noise. Moreover, due to the fact that most package AC were purchased for non-domestic uses, such as in stores and buildings that were already noisy, there was not much concern about noise. But as living standards rise, package AC are now found more frequently in average households, bringing noise reduction to the attention of manufacturers.

Generally, noises in AC can be categorized into two types: air-borne noises made by air flow, and structure-borne noises caused from the vibration of the structure. Structure-borne noise is from structural vibration, such as resonance from the structure, and has a lower frequency than air-borne noise. Due to these facts, general noise control solutions, such as sound insulation and absorption, are not effective ways to reduce noise. The more effective method to improve noise quality is to control structural vibration, which is the direct cause of noise. Because reducing air-borne noise alone has limited effects, research on controlling structure-borne noise caused by structural vibration from fans and motors is critical.

For these reasons, this study has been conducted with the interest of controlling structure-borne noise. The particular objective was to establish a low-noise low-vibration model for motor brackets using DOE.

2. CHARACTERISTICS OF VIBRATION-NOISE FOR INDOOR AIR-CONDITIONERS

2.1 Noise measurement of indoor air-conditioner while operating

Generally, noise from indoor air-conditioners in operation can be classified into air-borne noises, such as fluid noise from the refrigerant, vibro-noise from the thermal exchanger pin, blower passing frequency(BPF) of the fan; and structure-borne noises caused from vibration, such as radiation noise from the fan motor, 2f own magnetic-noise from motor vibration, resonance of the AC structures (motor bracket, cabinet, intake grill), and structural interference.

It shows that high sound-pressure levels in the noise-frequency spectrum are 120Hz and 500Hz. Here, the sound at 500Hz is the noise due to the air being cut-off from the fan blade, which is a BPF noise factor related to the number of fans and revolutions. The frequency with the strongest sound occurs around 120Hz and is directly radiated from the fan drive motor, which uses a 60Hz A.C. power source. Because the fan drive motor is driven with an A.C. power source, two torque ripples are generated during each revolution. It is a phenomenon similar to an incandescent electric lamp using a 60Hz A.C. power source that flickers 120 times per second. Therefore, motor magnetic noise of indoor AC occurs at 120Hz or 2nd, 3rd harmony ingredient and when this peak factor is high, it becomes a sound quality problem that results in a very unpleasant physical feeling. Because more unpleasant noise is caused by pulsation among these frequencies, it can become a serious problem.

2.2 Sound intensity measurement of indoor air-conditioners during operation

Sound intensity is defined by the vector product multiplied by the sound pressure, and particle velocity is the sound energy that passes through the unit from a given location as a ratio of changes per hour. In this study we will represent noise sources as measurements of AC sound intensity so that we can find the location of the main noise source at 120 Hz.

The measurements were taken on the back side of the cabinet (30cm) and the measurement points were considered aliasing of the space about 6*18, so it was established to 10cm distance. To locate the sound source at each frequency, we measured the radiation sound intensity of the

near field on the back side of the AC during operation.

Figure 1 and 2 show the measurement of sound intensity in a contour map. In the front surface, each picture shows that noises at 120Hz are concentrated on the right top position of the air conditioner and the bottom position of the intake grill and are the main noise sources. Consequently, noises at 120Hz come mainly from the motor section.

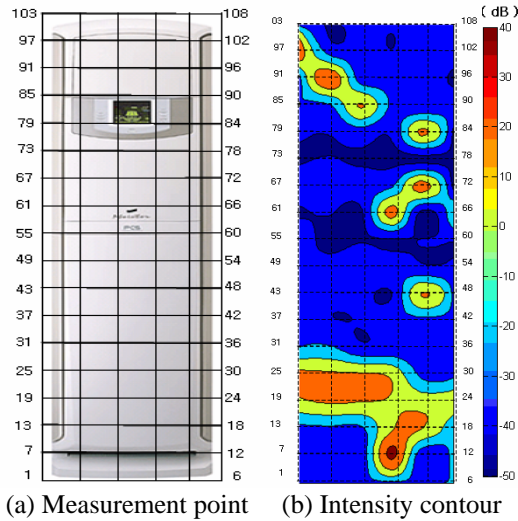


Figure 1. Sound intensity contour at the front cabinet

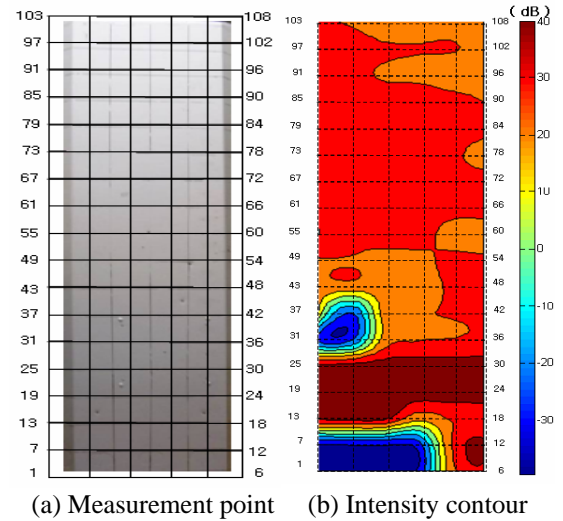


Figure 2. Sound intensity contour at the back cabinet

2.3 Operational deflection shape measurement of indoor air-conditioners

We defined the main parameters that determine sound level from the sound pressure spectrum of the AC and sound intensity distribution. To study the vibration pattern of these parameters, we measured the operational deflection shape (ODS) during AC operation.

In this experiment, after pre-test measurements of vibration on the backside of the AC cabinet, one of two accelerometers was attached to the point with the largest vibration point with a reference signal. The transfer function was measured by moving the position of another accelerometer. We measured about 18*5 points per 10cm, considering the bending wave in the interested frequency, and analyzed data with an auto-power spectrum of a single standard G-meter and a transfer function at each point. In the spectrum measurement results of the vibration signal on the backside of the AC cabinet, the high vibration value was 120Hz, as seen in Figure 3. This value agrees with the exciting frequency of the fan motor.

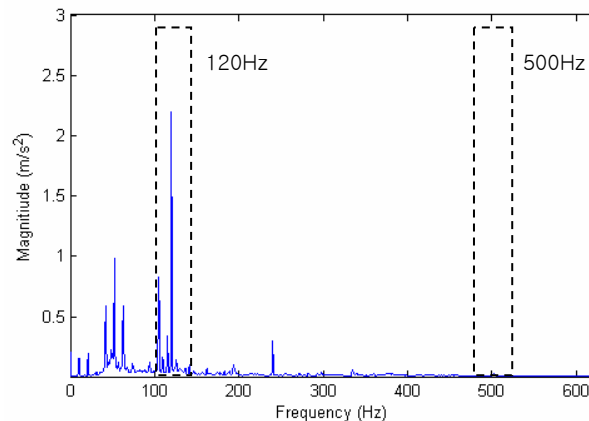


Figure 3. Vibration Spectrum at the back cabinet

On the other side, as compared with the results of the vibration spectrum and noise spectrum, the noise was 500Hz, which is BPF and does not contribute to cabinet vibration; there is no correlation between structure-borne noise and cabinet vibration.

The excitation of the motor influences the cabinet generally by emitting a high-pitched noise at 120Hz, as seen in Figure 1(b), which is the measurement result of the intensity. We found that the point at which high noise occurs is the same as the point at which high vibrations occur, when comparing the sound intensity results at 120Hz. This shows that the excitation of the motor can have a great effect on radiation noise and vibration in all aspects of the cabinet. Many methods for noise control can be used, including noise source control using a superior motor, transmission control through vibration isolation, and structural change and high stiffness design of the structure, etc.

2.4 Modal testing of the motor bracket

The motor bracket of the AC is a structural component that performs a role in fixing the motor and cabinet of the AC and isolating vibration. The bracket supports a motor, so the dynamic characteristics of the motor bracket are influenced by vibrations of the motor. The motor is fixed on the cabinet directly, so the bracket receives the dynamic load and transfers it to the cabinet while the motor is operating.

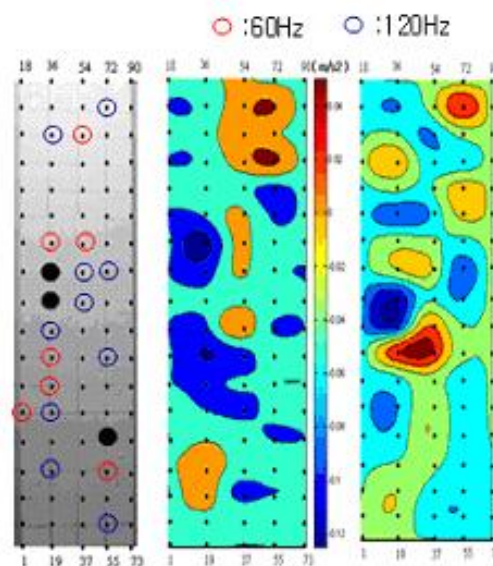


Figure 4. Operational deflection shape of the back cabinet

Vibration from the AC motor can cause problematic indoor noise. We performed modal testing to get the natural frequency and mode shape of the AC motor bracket. The experiment was performed to find the vibration mode by impulse force using an impact hammer in the actual boundary condition by which the motor bracket is assembled in the AC.

The experiment was performed using a PCB 086C02 impact hammer, PV-90B accelerometer made by RION, and an FFT analyzer made by Data Physics. According to the results, the natural frequency of the motor bracket is 125.5Hz which is close to 120Hz, the excitation frequency of the AC motor. The similarity of the natural frequency of the structure and the excitation frequency means that the resonance is generated when the external excitation transfers to the structure and the excessive vibration causes noise. Therefore, the resonance frequency of the AC motor bracket should be designed to avoid transferring external excitation to the driving frequency region of the motor.

3. DESIGN OF THE MOTOR BRACKET FOR NOISE REDUCTION USING DOE

In this study, we seek to determine the most appropriate design for reducing vibration and noise from the motor bracket, the noise source studied by the experiment. At first, an analysis model was created based on the previous bracket model and derived boundary conditions after an experiment with the actual bracket and cabinet. Using these boundary conditions, a new model was created to bead and hole and deduced variously. When each model was made by considering bead, hole, and thickness, we selected the most effective factors to reduce the number of simulations using DOE. Ultimately, we want to create a better design for controlling noise and vibration.

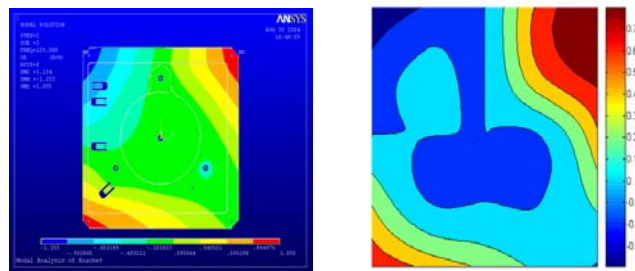
3.1 Modelling of the air-conditioner motor bracket

A SHELL63 elastic shell model, which has 6 degrees of latitude in each node point, was used as an element in the motor bracket of this experiment. The parts where the motor and the bracket are connected were modelled with BEAM4, which was the 3D BEAM element used after considering rigid body movement. Also, in this study the motor was modelled with MASS21 element after a consideration of static load. We assumed a finite element with isotropy, homogeneity, and linear elasticity.

3.2 Modal analysis and abstraction of boundary conditions of the air-conditioner's motor bracket

After modelling the bracket, we considered the mass (4.2kg) of the motor and performed the analysis. Also, before modal analysis we considered static deformation, determining which bracket is absorbing the motor's mass through pre-stress analysis.

The boundary conditions were decided before the modal analysis. Because the five parts connected with the bracket and cabinet on the actual AC are riveted, to make the model for the rivet connection region, boundary conditions of five parts were derived. Through the comparison of experimental and analysis results, given as exchanging the degree of freedom of the five parts using DOE with about six degrees of freedom for the node condition of rivet connection part, the most similar boundary condition was extracted. This boundary condition was applied to the new, improved model. Through this method, we selected an analysis model that can respond reliably and similarly to the real bracket model. Figure 5(a) shows the mode shape applied to the real boundary condition using FEM and Figure 5(b) shows the mode shape from the experimental result. We verified their similarity through analysis and experimental results.



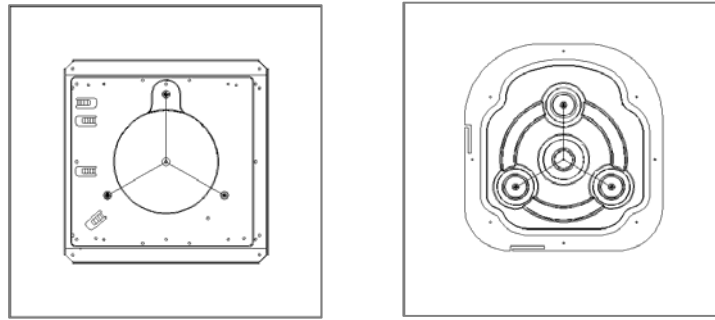
(a) FEM analysis result

(b) Experimental result

Figure 5. Comparison of modal analysis using FEM and experimental results of the bracket

3.3 Improved model of the air-conditioner motor bracket

Figure 6 shows the shape of the motor bracket that is used currently in air-conditioners and the newly designed motor bracket model. We designed a new model that can reduce manufacturing costs more than the previous model. We reinforced stiffness by putting beads on the part where the motor was connected. The motor was connected to the new model similarly to the previous model. The modal analysis for this new model was performed by considering the load of the motor and adding beads and holes by using DOE.



(a) Present model (b) Improved model
Figure 6. Comparison of the current model and improved model

3.4 Control factor effects for parameter design by using DOE

Figure 7 shows the modelling result of applying beads and holes to the new model. Beads were applied at 5 points and holes were applied at 8 points. Through the DOE, the optimum combination of beads and holes was determined for the model so that it had the farthest natural frequency in 120Hz driven frequency.

Each factor was as follows: Index A is the hole located at 330° clockwise around edge of the structure, B is at 30°, C is at 150°, and D is at 210°. Index E is the hole located at 330° in a clockwise direction around the center of the structure, F is at 30°, G is at 180°, H is at 0°. Index from now represents the direction of the bead, so I is at 330°, J is at 30°, K is at 90°, L is at 150°, M is at 240°. Finally, index N is the thickness of the bracket.

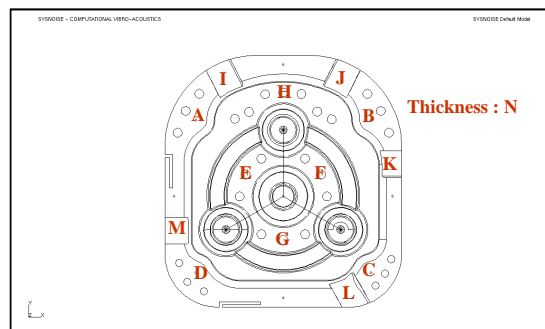


Figure 7. Overview of the motor bracket (factors)

In this study we used an orthogonal array with DOE to improve efficiency, because an advantage can result similar to that of full factorial design combination, minimizing the uses of fractional factorial design by using factor combination. Shape change factors of the motor bracket show 2 levels and 11 variables. The 2 levels develop irrespective of the beads and holes, and their thicknesses are 1.0mm or 1.2mm. From this, we selected an orthogonal array to

perform the process. We modified the model using factors and levels from the orthogonal array. Using FEM, we performed modal analysis. (Modal analysis considered the mass of motor.)

The optimum combination of position factors was found in index E (the hole is located at 330° in a clockwise direction) which removed the hole and N (thickness of bracket) was selected at 1.0mm (the bead and the hole remained). We designed the optimum combination and performed modal analysis.

As a result, the 125.5 Hz natural frequency of the previous model was changed to a 63.6Hz natural frequency. Because the natural frequency is so much lower than the driving frequency at 120Hz, the isolation of vibration in this model is more effective than in the previous model.

3.5 Verification of the improved model

Figure 8 shows the relation between the current model and the improved model. In the new model, the vibration of the motor is transferred to the motor bracket and cabinet, so it is isolated effectively. Figures 9 and 10 show the results as measurements of noise in the current model and the improved model in an anechoic room. And the overall sound pressure level of the measurement results shows that the sound at 120Hz is reduced to 4.7dB. So, the previous model in which the strongest sound occurred at 120Hz was controlled the noise effectively.

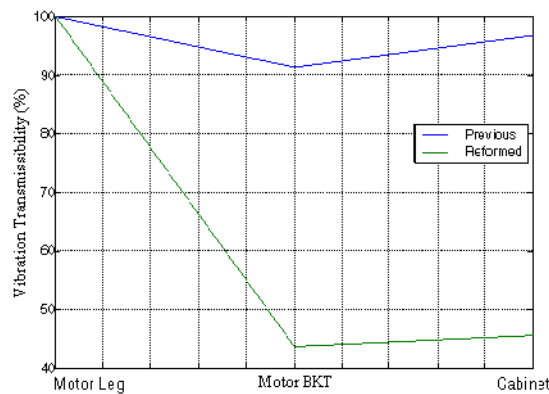


Figure 8. Vibration transmissibility ratio at 120Hz

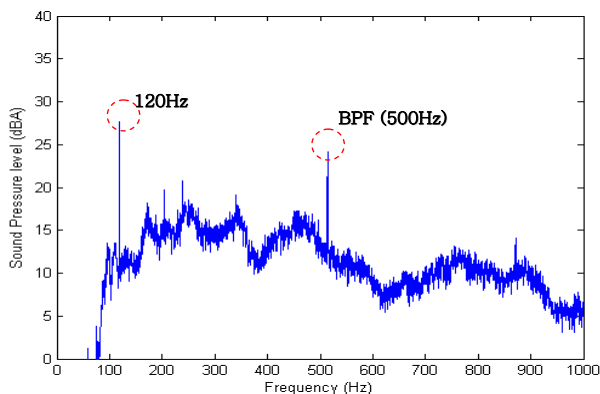


Figure 9. Sound pressure level of the current model

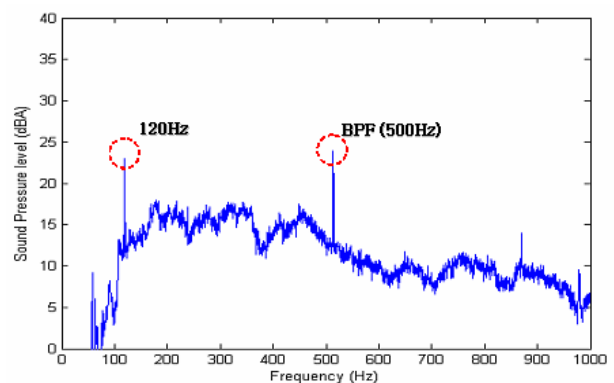


Figure 10. Sound pressure level of the improved model

4. CONCLUSIONS

We drew the following conclusions:

1. While air conditioners are operating, 120Hz and 500Hz are important noise frequencies for sound pressure level measurement. Also, it was confirmed by the frequency analysis that 120Hz is the driving frequency of the motor and 500Hz is the BPF (Blade Passing Frequency) frequency of the air conditioner fan.
2. While an air conditioner operated we examined closely the cause of noise with a sound intensity method that focused on important frequencies. We found that 120Hz components of the noise ranged from the lower part (motor region) to the top vice-whole of the air conditioner using a sound intensity experiment. It was predicted that the cause was the direct radiation of sound from the motor being discharged through the outlet and inlet port.
3. From the dynamic conduct measurements which used the vibration of the air conditioner and the ODS, the high vibration quantity is shown from the motor region. This phenomenon shows that by comparing intensity measurement results at 120Hz, the point where the highest sound occurs is the same as the point where the highest vibration occurs. Also, we found that the motor bracket has a 125.5 Hz natural frequency which is similar to the 120 Hz driving frequency of the air conditioner motor.
4. We performed a structural analysis of the current model with FEM and compared it with the test. The boundary conditions of the part connected to the cabinet were determined, applied to the proposed model, and examined for application possibilities. To find the improved model of sound vibration, we found the optimum combination of bracket beads and holes using a test plan by inserting various beads and holes. Since the bracket's natural frequency in the previous model was 125.5Hz, similar to the driving frequency of the motor, resonance could occur at these natural frequencies. After changing the bracket form, the natural frequency of the improved model became 63.6Hz which is far from that of the previous model. Thereby, in the new model, the possibility of resonance is reduced.

REFERENCES

- [1] F.J.Fahy, *Sound intensity*, 2nd E&FN SPON, 1989.
- [2] Frank J.Fahy, "Measurement of acoustic intensity using the cross-spectral density of two microphone signals", *JASA* **62**, pp1057-1059 (1977).
- [3] T.J.Schultz, "Measurement of acoustic intensity in reactive sound field", *JASA* **57**, pp.1263-1268 (1975).
- [4] Pavic,G., "Measurement of sound intensity", *JSV* **51**, pp533-546 (1977).
- [5] Chung,J.Y, "Cross-spectral method of measuring acoustic intensity without error caused by instrument phase mismatch" ,*JASA* **64**, pp1613-1616 (1978).
- [6] Adin Mann,J, "Instantaneous and time-averaged energy transfer in acoustic fields", *JASA* **82**, pp17~30 (1987).
- [7] Havard Vold, Brian Schwarz, Mark Richardson, *Display Operating Deflection shapes from Nonstationary data*, Sound and vibration, 2000.
- [8] McHargue, P.L, and Richardson, M.H., "Operating deflection shapes from time versus frequency domain measurements," *Proceedings of the 11th International Modal Analysis Conference*, Kissimmee, Florida, February, 1993.
- [9] J.S.Bendat and A.G.Piersol, *Random data : Analysis and Measurement Precedures*, New York: Wiley-Interscience, 1986.